Phytomedicine 125 (2024) 155350

Contents lists available at ScienceDirect

Phytomedicine

journal homepage: www.elsevier.com/locate/phymed

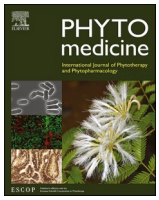

Original Article

Licochalcone A and B enhance muscle proliferation and differentiation by regulating Myostatin

Khurshid Ahmad [a,b,1], Eun Ju Lee [a,b,1], Shahid Ali [a,b], Ki Soo Han [c], Sun Jin Hur [d], Jeong Ho Lim [a,b], Inho Choi [a,b,*]

[a] Department of Medical Biotechnology, Yeungnam University, Gyeongsan 38541, South Korea
[b] Research Institute of Cell Culture, Yeungnam University, Gyeongsan 38541, South Korea
[c] Neo Cremar Co., Ltd., Seoul 05702, South Korea
[d] Department of Animal Science and Technology, Chung-Ang University, Anseong 17546, South Korea

ARTICLE INFO

Keywords:
Myostatin
Skeletal muscle
Licochalcone A
Licochalcone B
Myogenesis

ABSTRACT

Background: Myostatin (MSTN) inhibition has demonstrated promise for the treatment of diseases associated with muscle loss. In a previous study, we discovered that *Glycyrrhiza uralensis* (*G. uralensis*) crude water extract (CWE) inhibits MSTN expression while promoting myogenesis. Furthermore, three specific compounds of *G. uralensis*, namely liquiritigenin, tetrahydroxymethoxychalcone, and Licochalcone B (Lic B), were found to promote myoblast proliferation and differentiation, as well as accelerate the regeneration of injured muscle tissue.

Purpose: The purpose of this study was to build on our previous findings on *G. uralensis* and demonstrate the potential of its two components, Licochalcone A (Lic A) and Lic B, in muscle mass regulation (by inhibiting MSTN), aging and muscle formation.

Methods: G. uralensis, Lic A, and Lic B were evaluated thoroughly using *in silico, in vitro and in vivo* approaches. *In silico* analyses included molecular docking, and dynamics simulations of these compounds with MSTN. Protein-protein docking was carried out for MSTN, as well as for the docked complex of MSTN-Lic with its receptor, activin type IIB receptor (ACVRIIB). Subsequent *in vitro* studies used C2C12 cell lines and primary mouse muscle stem cells to acess the cell proliferation and differentiation of normal and aged cells, levels of MSTN, Atrogin 1, and MuRF1, and plasma MSTN concentrations, employing techniques such as western blotting, immunohistochemistry, immunocytochemistry, cell proliferation and differentiation assays, and real-time RT-PCR. Furthermore, *in vivo* experiments using mouse models focused on measuring muscle fiber diameters.

Results: CWE of *G. uralensis* and two of its components, namely Lic A and B, promote myoblast proliferation and differentiation by inhibiting MSTN and reducing Atrogin1 and MuRF1 expressions and MSTN protein concentration in serum. *In silico* interaction analysis revealed that Lic A (binding energy -6.9 Kcal/mol) and B (binding energy -5.9 Kcal/mol) bind to MSTN and reduce binding between it and ACVRIIB, thereby inhibiting downstream signaling. The experimental analysis, which involved both *in vitro* and *in vivo* studies, demonstrated that the levels of MSTN, Atrogin 1, and MuRF1 were decreased when *G. uralensis* CWE, Lic A, or Lic B were administered into mice or treated in the mouse primary muscle satellite cells (MSCs) and C2C12 myoblasts. The diameters of muscle fibers increased in orally treated mice, and the differentiation and proliferation of C2C12 cells were enhanced. *G. uralensis* CWE, Lic A, and Lic B also promoted cell proliferation in aged cells, suggesting that they may have anti-muslce aging properties. They also reduced the expression and phosphorylation of SMAD2 and SMAD3 (MSTN downstream effectors), adding to the evidence that MSTN is inhibited.

Conclusion: These findings suggest that CWE and its active constituents Lic A and Lic B have anti-mauscle aging potential. They also have the potential to be used as natural inhibitors of MSTN and as therapeutic options for disorders associated with muscle atrophy.

Abbreviations: ACVRIIB, activin type IIB receptor; CTX, cardiotoxin; CWE, crude water extract; FBS, fetal bovine serum; FMOD, fibromodulin; GAPDH, glyceraldehyde 3-phosphate dehydrogenase; G. uralensis, *Glycyrrhiza uralensis*; HRP, horseradish peroxidase; LicA, Licochalcone A; LicB, Licochalcone B; LicC, Licochalcone C; MSCs, muscle satellite cells; MYH, myosin heavy chain; MYL2, myosin light chain; MSTN, Myostatin; P/S, Penicillin/Streptomycin; SM, skeletal muscle; TGF-ß, transforming growth factor-beta.

* Corresponding author at: Department of Medical Biotechnology, Yeungnam University, Gyeongsan 38541, South Korea.
E-mail address: inhochoi@ynu.ac.kr (I. Choi).

[1] These authors contributed equally to this work.

https://doi.org/10.1016/j.phymed.2024.155350
Received 19 August 2023; Received in revised form 4 January 2024; Accepted 8 January 2024
Available online 9 January 2024

Introduction

Skeletal muscle (SM) is the most abundant body tissue and is essential for movement, posture, and body temperature regulation as well as for the physical protection of internal organs and soft tissues (Mukund and Subramaniam, 2020). Furthermore, SM has the potential to regenerate in response to injuries or disease conditions due to the presence of muscle satellite cells (MSCs, aka myogenic stem cells). MSCs are located between the sarcolemma and basal lamina and have the ability to self-renew and produce differentiated descendants (Kuang et al., 2008; Yin et al., 2013). MSCs typically remain quiescent; however, upon encountering tissue injury, they undergo asymmetric division to generate new stem cells and proliferating myoblasts. These myoblasts subsequently undergo differentiation into myocytes, which subsequently fuse and undergo maturation to form myofibers (Pang et al., 2023; Sousa-Victor et al., 2022). The organized regulation of transcription factors is essential for the proliferation and differentiation of MSCs into myotubes through the myogenic program (Hernández--Hernández et al., 2017).

Myostatin (MSTN) belongs to the transforming growth factor-beta (TGF-ß) family and is a negative regulator of muscle growth (Thomas et al., 2000), and thus plays a significant role in regulating MSC proliferation and differentiation. Furthermore, MSTN inhibition provides a promising strategy for the management of muscle-wasting diseases as the correlation between MSTN and muscle-wasting disorders is well-documented (Furrer and Handschin, 2019; Lee, 2021). Muscle wasting is allied with cancer-associated cachexia, sarcopenia, and a range of metabolic disorders, including obesity and diabetes (Argilés et al., 2006). Ubiquitin-mediated proteolysis is induced by MSTN and is one of the processes that lead to muscle atrophy in cancer cachexia (Liu et al., 2019). MSTN levels are elevated in the elderly and have an inverse correlation with lean muscle mass, implying that MSTN plays a role in age-related muscle decline (Baig et al., 2022).

Previously, we investigated the possibility of using SM mass as a biomarker of numerous diseases, including diabetes, obesity, and aging (Ahmad et al., 2023; Lee et al., 2018, 2022). Several extracellular matrix proteins, notably fibromodulin (FMOD), decorin, fibronectin, and lamininis, interact/bind to MSTN and modulate its function (Lee et al., 2021a, 2018; Miura et al., 2010). Also, *in vitro* and *in silico* studies have revealed that FMOD binds to MSTN and prevents it from interacting with its native receptor ACVRIIB (activin type IIB receptor). Notably, FMOD significantly reduced the MSTN -ACVRIIB interaction and thereby promoted myogenesis (Lee et al., 2021b). Other studies examined how MSTN expression affects muscle mass and currently, there is much interest in creating anti-MSTN therapeutics to prevent muscular atrophy (Abati et al., 2022; St. Andre et al., 2017; Welle et al., 2009). Several trials on MSTN inhibitors were discontinued at the phase 1 level due to lack of efficacy (MYO-029/Stamulumab, PF-06252616/Domagrozumab), but a few candidates successfully completed phase 2 trials and are undergoing further development (2495655/Landogrozumab, REGN-1033/Trevogrumab, SRK-015)(Baig et al., 2022; Rybalka et al., 2020; Suh and Lee, 2020). Additionally, the ligand traps ACE-031 and ACE-083, which were created by Acceleron, function in a distinctive manner within the TGF-β superfamily. ACE-031 functions by mimicking the ACVR2B receptor and combining its ligand-binding section with an immunoglobulin Fc domain. However, ACE-083 merges a portion of the binding protein FST with an Fc domain. Both biologics demonstrate flexibility in their ability to bind to a wide range of TGF-β superfamily members, including MSTN, GDF-11, activins, and particular BMPs (Lee et al., 2023).

Novel drug development continues to rely heavily on natural products. In fact, up to 60 % of small-molecule medications approved during the last 2, 3 decades were derived in this manner (Atanasov et al., 2021; Newman and Cragg, 2012). A plethora of natural compounds, including Epigallocatechin-3-gallate and others, have been extensively researched due to their diverse therapeutic effects (Chu et al., 2017a, 2017b, 2019). Furthermore, studies on natural compounds that target MSTN have identified compounds with significant inhibitory activities, such as Epicatechin (Gutierrez-Salmean et al., 2014; Mafi et al., 2019), Fructus Schisandrae (Kim et al., 2015), Sulforaphane (Fan et al., 2012), Astragalus polysaccharide (Liu et al., 2013), and others. Recently our *in silico* investigations showed that curcumin and gingerol might potently inhibit MSTN by inhibiting MSTN-ACVRIIB binding (Baig et al., 2017). In addition, a virtual screening analysis showed two natural compounds in traditional Chinese medicines (Ali et al., 2022), and dithymoquinone (Ahmad et al., 2021) from another natural compound library effectively inhibit MSTN.

Glycyrrhiza uralensis (G. uralensis, licorice) is a well-known herb in traditional Chinese medicine, and its bioactive components exhibit a wide range of pharmacological properties, including anti-inflammatory, anti-allergic, antioxidant, anticancer, and neuroprotective properties (Asl and Hosseinzadeh, 2008; Ayeka et al., 2016). In our recent studies on *G. uralensis*, we found that its water extract inhibits MSTN expression and promotes myogenesis and that three compounds, namely liquiritigenin, Lic B, and tetrahydroxymethoxychalcone increase myoblast proliferation and differentiation and accelerate injured muscle regeneration (Lee et al., 2021c). To extend this research, we investigated, in more detail, the abilities of two components of *G. uralensis, viz.* Lic A and B, to regulate muscle mass, aging, and myogenesis using *in silico, in vitro,* and *in vivo* approaches.

Materials and methods

In silico analysis

Protein-ligand and protein-protein docking

The 3D structure of MSTN (PDB ID: 3HH2) was obtained from the protein data bank, and after removing heteroatoms and water molecules, the MSTN monomer was prepared using Discovery Studio 2022 (DS) for molecular docking studies. Auto Dock 4.2 (Morris et al., 2009) was used for site-specific docking of three components of *G. uralensis*, namely Lic A, Lic B, and Lic C (Supplementary Fig. 1) into the active site of MSTN. The XYZ coordinates for the active site as set as -20.387444 -14.867815 60.168148, respectively. Further, the 3D structure of ACVRIIB (PDB ID: 1S4Y) was retrieved and used in a protein-protein interaction (PPI) study. PPI studies on interactions between MSTN and ACVRIIB and between MSTN -Lic A, -Lic B, or -Lic C complexes and ACVRIIB, were carried out using the PatchDock web server (Schneidman-Duhovny et al., 2005) and refined and ranked using FireDock (Mashiach et al., 2008). The best complex poses were used in the final analysis. The visualization tools PyMOL (Yuan et al., 2017) and DS were used to perform all visual assessments of docking results.

Molecular dynamics simulations

Lic A- MSTN, Lic B- MSTN, and Lic C- MSTN were subjected to molecular dynamics (MD) simulations using GROMACS 2019. 6 (Van Der Spoel et al., 2005) and the GROMOS96 43a1 force field (Pol-Fachin et al., 2009). The 'particle-mesh Ewald' method was employed to analyze interactions between MSTN and Lic A, B, and C. The MD system was then minimized using the steepest descent method (1500 steps). NVT and NPT ensembles were used to complete the equilibration process in two steps. The examination of MD trajectories using GROMACS analysis modules was conducted after the completion of the final production phase, which lasted for 100 ns, at a temperature of 300 K. Visual molecular dynamics (VMD) (Humphrey et al., 1996) and PyMOL was used to create graphical representations of the 3D models.

Mouse experiment

C57BL/6 male mice, aged 6 weeks, were obtained from Hyochang Science (Daegu, Korea). They were kept in groups of four per cage in a temperature-controlled room. The mice were fed a standard diet (4.0 % (w/w) total fat). All animal-related experiments were performed according to the guidelines issued by the Institutional Animal Care and Use Committee of Yeungnam University (YU-IACUC-2022-013, 2022-Mar-01). To examine the effects of the CWE of *G. uralensis* (hereafter CWE), Lic A (Sigma Aldrich, St. Louis, Mo, USA, empirical formula: $C_{21}H_{22}O_4$, purity: ≥96.0 %, molecular weight: 338.40), or Lic B (ChemFaces, Wuhanm China, empirical formula: $C_{16}H_{14}O_5$, purity: ≥98.0 %, molecular weight: 286.28) on muscle, six-month-old mice were orally administered CWE (100 mg/kg), Lic A (3 mg/kg), or B (3 mg/kg) daily for 14 (CWE) or 11 days (Lic A and B). Mice were anesthetized with Avertin i.p. (Sigma Aldrich) after 14 or 11 days of administration, and gastrocnemius (gas) muscle tissues and plasma have been obtained for analysis.

CTX injection and CWE administration

Cardiotoxin (CTX) and CWE were administered as previously described (Lee et al., 2021c).

Western blot

The Western blotting procedure was carried out as it had been previously detailed (Lee et al., 2019).

60 μg of extracted protein was electrophoresed and transferred to PVDF membranes. These membranes were subsequently incubated in blocking reagent and subjected to overnight treatment with primary antibodies [MSTN (1:1000), MYH (1:500), MuRF1 (1:500), Atrogin1 (1:500), ACVRIIB (1:500), Ki67 (1:500) β-actin (1:1000) (Santa Cruz Biotechnology), MYL2 (1:1000), or CyclinA2 (1:500) (Abcam, MA, USA) (gas) antibodies] in 1 % skim milk or BSA in TBS at 4 °C. After washing, membranes were incubated for 1 hr at room temperature with goat-rabbit or mouse-horseradish peroxidase (HRP)-conjugated secondary antibodies (Santa Cruz Biotechnology), and blots were visualized using Super Signal West Pico Chemiluminescent Substrate (Thermo Fisher Scientific).

Phalloidin staining

Muscle tissue sections were deparaffinized, hydrated, quenched, and stained with phalloidin (1:400, Invitrogen, Carlsbad, CA, USA). A fluorescence microscope equipped with a digital camera was used to capture images.

H&E staining and muscle fiber diameters

The H&E staining and subsequent muscle fiber diameter measurements followed previously established protocols (Schneider et al., 2012). In brief, paraffin-embedded sections were deparaffinized with xylene, rehydrated using an ethanol series, stained with H&E, and examined under a light microscope. The diameters of the muscles were measured utilizing the Image J software.

Immunohistochemistry

The immunohistochemistry procedure was carried out in accordance with the previously described methodology (Lee et al., 2019). Briefly, muscle tissue sections were deparaffinized, hydrated, quenched, and blocked with 1 % normal goat serum. Sections were then incubated with MSTN (1:50), atrogin1 (1:50), MuRF1 (1:50), ACVRIIB (1:50), and laminin (1:50, Invitrogen, MA, USA) antibodies overnight at 4 °C and treated with HRP-conjugated antibody (1:100, Santa Cruz Biotechnology) or Alexa Fluor 594 goat anti-mouse secondary antibodies (1:100; Thermo Fisher Scientific) at room temperature for 1 h.

Immunocytochemistry

The immunocytochemistry protocol was carried out in accordance with the established methodology described in previous papers (Lee et al., 2019). In brief, following fixation with formaldehyde, the cells were subjected to an incubation period of 5 min with 0.2 % Triton X-100. Subsequently, the cells were rinsed with PBS and incubated with 1 % normal goat serum for an additional 30 min prior to their incubation with protein-specific primary antibodies [MYL2 (1:50), or MYH (1:50)] at 4 °C overnight. Alexa Fluor 488 or 594 goat anti-rabbit or anti-mouse secondary antibodies (1:100; Thermo Fisher Scientific) were then added and incubated for 1 hr at room temperature. Cells were then stained with DAPI (Sigma-Aldrich) and imaged under a fluorescence microscope.

Myostatin ELISA

An MSTN ELISA kit (R&D Systems NE, Minneapolis, MN, USA) was used to measure plasma MSTN protein concentrations. Briefly, plasma was added to antibody-coated plates and incubated at room temperature for 90 min. After removing the top phase, antibodies were added, and plates were incubated at room temperature for 1 h. The plates were then rinsed, the enzyme conjugate was added, and the plates were incubated at 37 ℃ for 30 min. The substrate was introduced after unbound substances were eliminated via rinsing, and the reaction was left to continue for a duration of 15 min. Utilizing a Versa Max microplate reader (Tecan Group Ltd., Mannedorf, Switzerland), absorbance was assessed at 450 nm after the addition of the stop solution.

Mouse MSCs isolation

Mouse MSCs were isolated as previously described (Lee et al., 2021c).

Mouse MSCs and C2C12 cell proliferation

Murine C2C12 myoblast cells (Korean Cell Line Bank, Seoul, Korea) and mouse MSCs were cultured in growth media [C2C12 cells in DMEM (HyClone Laboratories, South Logan, UT, USA) + 10 % FBS (fetal bovine serum, HyClone Laboratories) + 1 % P/S (Penicillin/Streptomycin, Thermo Fisher Scientific, Waltham, MA, USA), and mouse MSCs in Ham's F10 (HyClone Laboratories)+10 %FBS+1 %P/*S*+mouse FGF2 (fibroblast growth factor 2, 5 ng, Milteny Biotec, Bergisch Gladbach, Germany)] in a humidified 5 % CO_2 incubator at 37 ℃. To determine the effects of CWE, Lic A,B, and C (Sigma Aldrich, empirical formula: $C_{21}H_{22}O_4$, purity: ≥90.0 %, molecular weight: 338.40), cells were incubated with growth media supplemented with CWE (100 ug/ml), Lic A, Lic B (1 ng/ml), or Lic C (1, 5, and 10 ng/ml) for 1 day.

Differentiation of mouse MSCs and C2C12 cells

When MSCs or C2C12 cells reached 100 % confluence, growth media was replaced with differentiation media (DMEM+2 %FBS+1 %P/S) containing 1 ng/ml Lic A or Lic B (Sigma Aldrich, St Louis, MO, USA) for 2 or 4 days.

Ceramide treatment and compound treatment

C2C12 cells were cultured with growth media supplemented with 50 μM ceramide (Sigma Aldrich) for 2 days and then 1 day later incubated with growth media supplemented with CWE (100 ug/ml), Lic A, or Lic B (1 ng/ml) for 2 days.

Cell cycle analysis

FACS was used to analyze cell cycles. Control and ceramide-treated cells were trypsinized, centrifuged, and collected. Cell cycle analysis was performed as previously described (Langley et al., 2002).

Creatine kinase analysis

Cells were collected and washed with PBS and centrifuged at 1000xg for 15 min. Supernatants were analyzed using a creatine kinase assay kit (BioAssay Systems, CA, USA). Creatine levels were calculated as follows;

$$\mathrm{CK(U/L)} = \frac{\mathrm{O.D40min} - \mathrm{O.D20min}}{\mathrm{O.D\,CALIBRATOR} - \mathrm{O.DH2O}} \mathrm{X600}$$

MTS assay

Cell culture media were removed, and cells were cultured in growth media supplemented with CellTiter 96 Aqueous One Solution Reagent (Promega, WI, USA) for 1 h in a humidified 5 % CO_2 incubator at 37°C. Absorbances were measured at 490 nm using a Versa max microplate reader (Tecan Group Ltd., Mannedorf, Switzerland).

Real time RT-PCR

The real-time RT-PCR was performed according to the methods previously described (Lee et al., 2021c). Supplementary Table S1 provides primer information.

Statistical analysis

The T-test and Tukey's Studentized Range test were used to examine the significance of differences between mean normalized gene and protein expressions. GAPDH or β-actin were used as internal controls, and the analysis was performed using one-way ANOVA in SAS ver. 9.0 (SAS Institute, Cary, NC, USA). Statistical significance was accepted for P values < 0.05.

Results

In silico interactions between Licochalcones, Myostatin, and ACVRIIB

Molecular docking was used to evaluate the effects of Lic A, B, or C on the binding efficiency of MSTN with its native receptor ACVRIIB and the docking of MSTN-Lic A, Lic -B, and -Lic C complexes with ACVRIIB. Molecular docking showed the average binding energies of Lic A, B, or C with MSTN were -6.9, -5.9, and -6.8 kcal/mol, respectively (Fig. 1A). The predicted average inhibition constant (pKi) based on the binding energies was determined to be 237.15, 261.86, and 1077.26 μM for the docked complexes of Lic A, B, and C with MSTN, respectively (Supplementary Table S2). Protein-protein docking of MSTN with ACVRIIB was performed with or without Lic A, B, or C. The binding energy of MSTN-ACVRIIB complex, in terms of global energy, was -59.97 kcal/mol, and those of LicA- MSTN-ACVRIIB, Lic B-MSTN - ACVRIIB, and Lic C-MSTN -ACVRIIB were -52.71, -56.78, and -51.38, respectively, which demonstrated that in the presence of Lic A, B, and C, the binding efficiencies of MSTN with its receptor were reduced (Fig. 1).

The stability profiles of Lic A-, Lic B-, and Lic C-MSTN complexes were monitored throughout simulation runs to determine their relative root-mean-square deviations (RMSDs), which are commonly used to calculate spatial deviations of groups of atoms from a reference structure. Mean RMSD values of complexes Lic B-MSTN, and Lic C-MSTN were 0.49 and 0.45 nm, respectively, and Lic A-MSTN had a value of 0.61 nm (Fig. 2A). Initially, all three complexes exhibited stable conformations, but after 60 ns Lic A-MSTN had a slightly elevated RMSD. Ligand dynamics in the catalytic pocket of MSTN were also explored, and trajectories revealed that all three ligands (Lic A, Lic B, and Lic C) displayed similar interaction patterns (Fig. 2B). Interestingly, Lic B-MSTN and Lic C-MSTN complexes bound more stably in the catalytic pocket of MSTN (Fig. 2C). Root-mean-square fluctuation (RMSF) plots

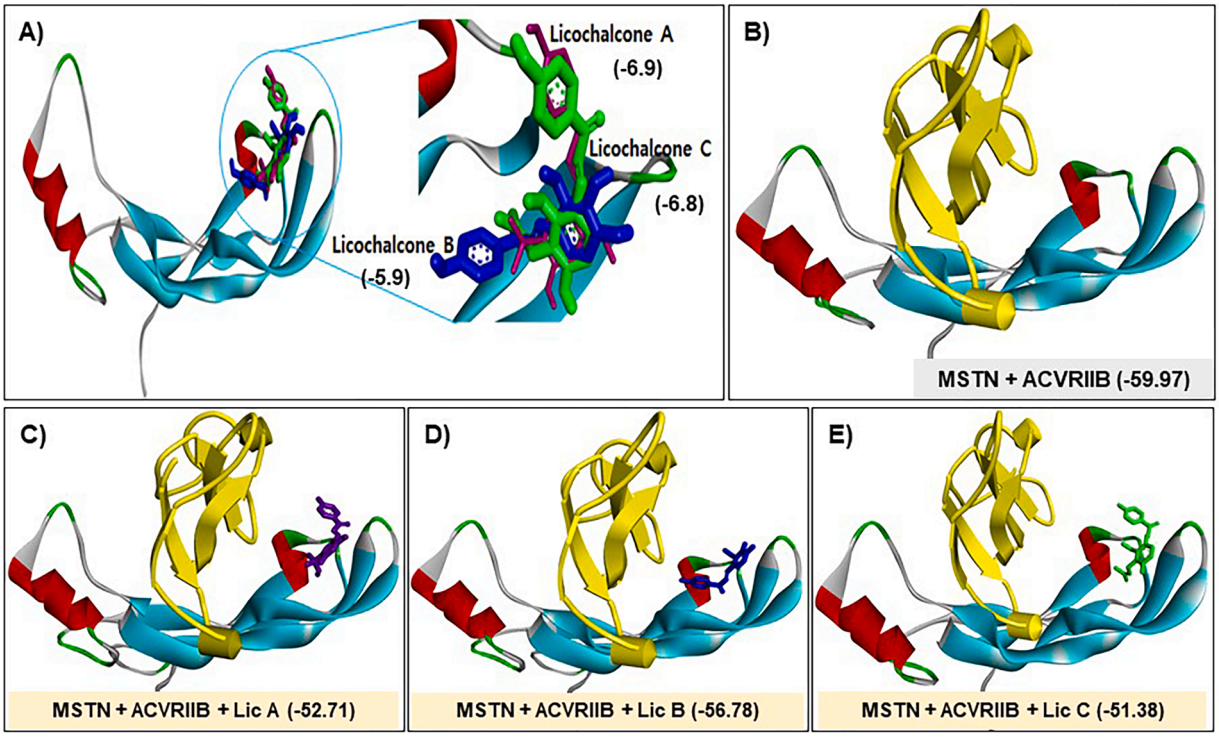

Fig. 1. Interactions between Licochalcones, MSTN, and ACVRIIB. (A) Interactions of Lic A, B, and C in the binding pocket of MSTN, (B) Interaction between MSTN and ACVRIIB, C) Interaction between MSTN-Lic A complex and ACVRIIB, (D) Interaction between MSTN-Lic B and ACVRIIB and (E) Interaction between Myostatin-Lic C and ACVRIIB.

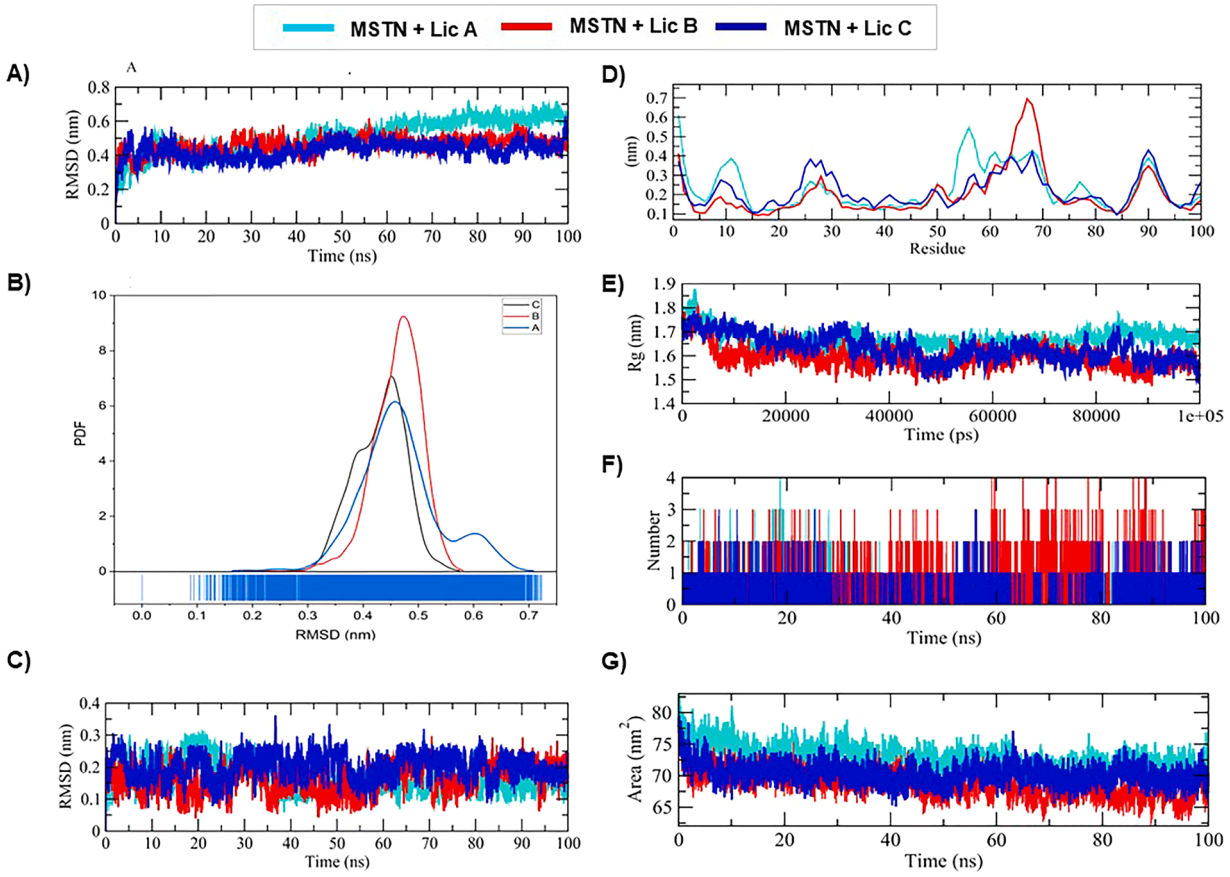

Fig. 2. Conformational studies of docked complexes (MSTN+Lic A, MSTN+Lic B, and MSTN+Lic C). (A) RMSD plot of complexes, (B) probability distribution function plot, (C) RMSD plot of ligands, (D) RMSF plot of backbone, (E) Radii of gyration, (F) Numbers of H-bonds in complexes, (G) SASA plots.

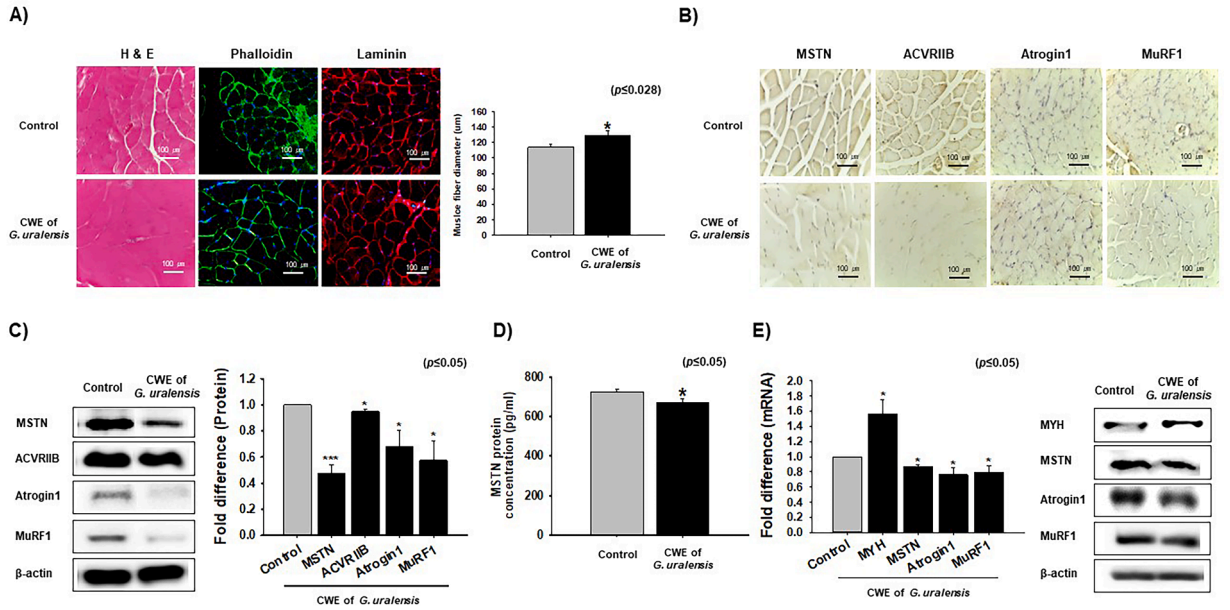

Fig. 3. Effect of CWE on mouse gastrocnemius muscles. Mice were orally treated with the CWE of *G. uralensis* (CWE, 100 mg/kg) daily for 14 days and gastrocnemius muscle tissues were collected from non-treated (Control) and treated mice. (A) Muscle tissues were stained with H&E, phalloidin, and laminin, and muscle fiber diameters were determined using Image J. (Green: Phalloidin, Red: Laminin, Blue: DAPI) (B) Expressions of MSTN, ACVRIIB, Atrogin1, and MuRF1 were assessed by immunohistochemistry in non-treated and treated muscles. (C) MSTN, ACVRIIB, Atrogin1, and MuRF1 expressions were analyzed by Western blot and assessed using Image J. (D) Plasma MSTN concentrations were measured by ELISA. (E) MSCs were isolated from gastrocnemius muscles. When MSCs reached 100 % confluency, media were replaced with differentiation medium supplemented with CWE (100 ug/ml) and incubated for 2 days. MYH, MSTN, Atrogin1, and MuRF1 mRNA and proteins expressions were analyzed by real time RT-PCR and Western blot, respectively. Results are presented as means±SDs (n = 7–12). * $p \leq 0.05$, ** $p \leq 0.001$, *** $p \leq 0.0001$.

were used to identify interacting residues and revealed all complexes were stable (Fig. 2D). In addition, radii of gyration (Rg) were evaluated to determine the compactnesses of complexes, and Rg plots showed that Lic B-MSTN and Lic C-MSTN were more compact than Lic A-MSTN (Fig. 2E). Hydrogen (H) bond analysis was used to characterize binding interaction patterns. Lic A and Lic B formed 2–4 H bonds with the active pocket of MSTN, whereas Lic C formed 1, 2 H bonds (Fig. 2F). Furthermore, the solvent-accessible surface areas (SASAs) of Lic B-MSTN and Lic C-MSTN were smaller than those of Lic A-MSTN (Fig. 2G). Collectively, the *in silico* study showed that Lic A, Lic B, and Lic C bind MSTN in a stable and essentially identical manner.

CWE effects on normal muscle tissue and primary MSCs

CWE was orally administered to C57BL/6 mice for 14 days. Muscle fiber diameters were then measured after H&E, phalloidin (membrane), and laminin staining of control and CWE-treated muscles. CWE-treated mice had significantly larger muscle fiber diameters (129 μm) than controls (114 μm) (Fig. 3A). Immunohistochemistry and Western blot were used to assess MSTN, ACVRIIB, Atrogin1, and MuRF1 levels to investigate the mechanism of CWE-induced muscle growth. Muscles treated with CWE contained significantly lower levels of these proteins (Fig. 3B, C). Furthermore, plasma MSTN levels were considerably lower in CWE treated mice (647.2 pg/ml) than in normal controls (708.2 pg/ml) (Fig. 3D). These findings suggest that the inhibition of MSTN and atrophy-related genes by CWE was probably the cause of the observed reduction in muscle fiber diameter.

The activity of creatine kinase, which is elevated in injured muscle tissues, was measured and found to be significantly lower in the plasma of CWE-treated mice than in untreated controls (Supplementary Fig. 2). Furthermore, MSTN, Atrogin1, and MuRF1 mRNA and protein expressions were significantly lower in CWE-treated mouse MSCs cultured in differentiation media for two days, whereas MYH mRNA and protein levels were increased by CWE treatment (Fig. 3E). These findings indicate that CWE promotes muscle growth by reducing the expressions of genes and proteins that induce muscle atrophy but upregulates MYH, which stimulates muscle cell development and enhances MSC differentiation.

Impact of Lic A and B on normal muscle tissues and primary MSCs

Lic A or B was administered orally to mice at 3 mg/kg daily for 11 days and muscle fiber diameters of excised gastrocnemius muscles were measured after H&E, phalloidin (membrane), and laminin staining. The mean muscle fiber diameters of Lic A and Lic B treated mice were 126.9 and 122.1 μm, respectively, which were both significantly greater than the control value (101.5 μm) (Fig. 4A). Immunohistochemistry and Western blot were used to assess MSTN, ACVRIIB, Atrogin1, and MuRF1 levels to investigate the roles played by Lic A and Lic B in muscle mass regulation. Treatments with Lic A or B were found to significantly reduce the levels of these proteins and increase muscle dimensions *versus* controls, which suggested Lic A and B enhance muscle growth by suppressing the expression of proteins that induce muscular atrophy (Fig. 4B, C). To explore the effects of Lic A or B on MSC differentiation, isolated mouse primary MSCs were treated with Lic A or B in a differentiation media for 2 days. These treatments substantially reduced MSTN, atrogin1, and MuRF1 levels, but significantly increased MYH levels (Fig. 4D). These findings indicate that Lic A and B regulate muscle mass as effectively as CWE.

CWE, Lic A, and Lic B effects on C2C12 myoblast proliferation

C2C12 cells were incubated in growth media containing CWE, Lic A, or Lic B for one day to investigate their effects on C2C12 cell proliferation. CWE treatment significantly increased proliferation, and this was accompanied by substantial increases in the expressions of the proliferation markers Ki67 and CyclinA2 at the mRNA and protein levels *versus* controls. Conversely, the mRNA and protein levels of MSTN, atrogin1, and MuRF1 were significantly reduced at the mRNA and protein levels. These findings indicate that CWE promotes cell

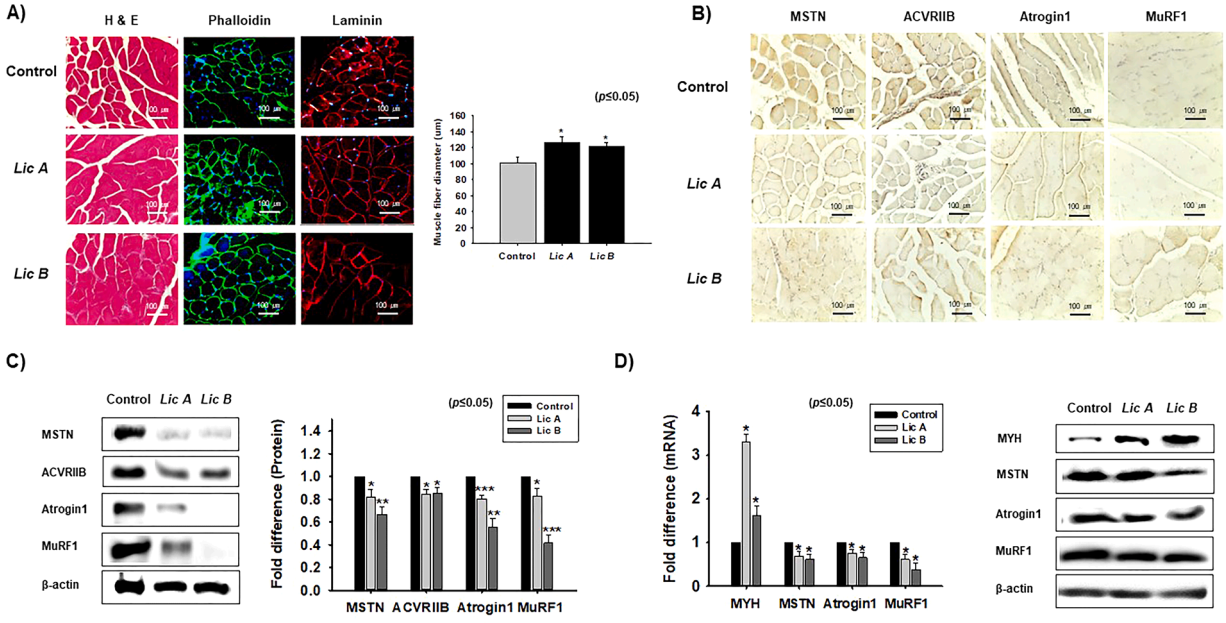

Fig. 4. Effects of Lic A and B on muscle. C57BL/6 Mice were orally treated with Lic A or B (3 mg/kg) once daily for 11 days and gastrocnemius tissues were collected from non-treated (Control) and treated mice. (A) Muscle tissues were stained with H&E, phalloidin, and (or?) laminin. Muscle fiber diameters in non-treated and treated muscles were assessed by Image J. (B) MSTN, ACVRIIB, Atrogin1, and MuRF1 protein levels were assessed by immunohistochemistry in non-treated and treated muscles. (C) MSTN, ACVRIIB, Atrogin1, and MuRF1 protein levels were determined by Western blot in non-treated and treated mice using Image J. (D) MSCs were isolated from mouse gastrocnemius muscles. When MSCs reached 100 % confluency, media were replaced with differentiation media supplemented with Lic A or B (1 ng/ml) and incubated for 2 days. MYH, MSTN, Atrogin1, and MuRF1 mRNA and proteins expressions were determined by real time RT-PCR and Western blot, respectively. Results are presented as means±SDs ($n = 6$). * $p \leq 0.05$, ** $p \leq 0.001$, *** $p \leq 0.0001$.

proliferation and suppresses the expressions of MSTN, Atrogin1, and MuRF1 (Fig. 5A). Likewise, when cells were treated with Lic A, Ki67 and CyclinA2 expressions increased whereas those of MSTN, Atrogin1, and MuRF1 decreased (Fig. 5B). The effects of Lic B were similar to those of CWE and Lic A, except for a relative decrease in Ki67 mRNA expression (Fig. 5C). CWE, Lic A, and Lic B treatment also reduced the expressions of SMAD2 and SMAD3 and eventually decreased phosphorylated SMAD2 and SMAD3 levels (Fig. 5D, E). SMAD 2 and 3 are intracellular signaling molecules and participate in the TGF-β/Smad pathway, which is involved in muscle mass regulation (Hata and Chen, 2016). These findings collectively indicate that CWE, Lic A, and B promote cell proliferation by downregulating the gene and protein expressions of MSTN and SMAD2/3 while upregulating those of Ki67 and CyclinA2.

Differentiation of C2C12 cells in response to Lic A and B

Previously, we noticed that CWE significantly increased C2C12 cell differentiation (Lee et al., 2021c). In this study, we investigated how Lic A and Lic B impacted C2C12 cell differentiation by incubating cells with Lic A-supplemented differentiation media and staining for MYL2 and MYH to observe myotube formation. Lic A treatment for 4 days increased MYL2, MYH, and creatine kinase levels (Fig. 6A, B), but reduced MSTN, Atrogin1, and MuRF1 levels (Fig. 6C), and treatment with Lic B treatment also increased MYL2, MYH, and creatine kinase levels (Fig. 6D, E). mRNA and protein expression analysis consistently demonstrated that LicA and Lic B had similar effects on MYL2, MYH, MSTN, Atrogin1, and MuRF1 (Fig. 6F). In addition, SMAD2 and SMAD3 expressions, and phosphorylated SMAD2 levels were lower in Lic A or Lic B treated cells than in controls (Fig. 6G, H). These findings suggest that Lic A and Lic B promote muscle differentiation in C2C12 cells, which is in line with observed increases in myotube formation, myogenic marker upregulations, and downregulations of MSTN, Atrogin1, and MuRF1. Furthermore, suppression of SMAD2 and 3 and their phosphorylated forms further supports the inhibition of MSTN by Lic A and Lic B, and their promotion of myogenic differentiation.

Lic C effects on C2C12 proliferation and differentiation

In silico analysis showed the effect of Lic C was similar to those of Lic A and B. To investigate the effect of Lic C on proliferation and differentiation, C2C12 cells were incubated in proliferation or differentiation media supplemented with Lic C for 1 or 4 days, respectively. Lic C treatment at 1 and 5 ng/ml had no meaningful effect on C2C12 proliferation or differentiation, but at 10 ng/ml it significantly decreased cell proliferation (Supplementary Figs. 3A and B). The *in silico* analysis revealed that Lic A, B, and C bind to MSTN in a comparable manner. Lic A and B showed significant *in vitro* results that were consistent with the *in silico* results, whereas Lic C did not exhibit comparable effects.

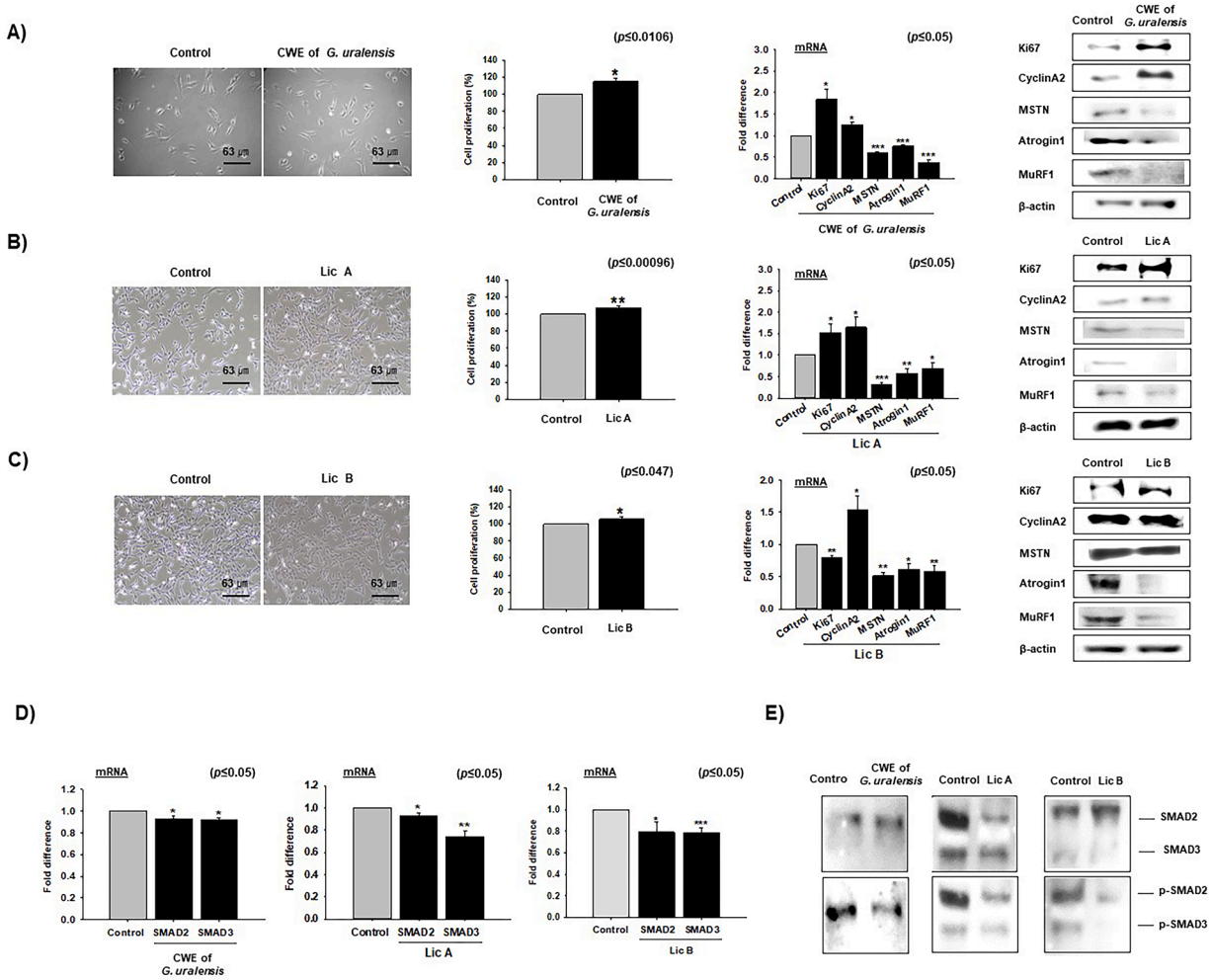

Fig. 5. Effects of CWE, Lic A, and B on myoblast proliferation. C2C12 cells were incubated in proliferation media supplemented with the CWE of *G. uralensis* (CWE) (100 ug/ml), Lic A, or Lic B (1 ng/ml) for 1 day. (A)–(C) Treated and non-treated cell proliferations were determined using an MTS assay. Ki67, Cyclin A2, MSTN, Atrogin1. and MuRF1 mRNA and proteins expressions were determined by real time RT-PCR and Western blot, respectively. (D) & (E) Effects of CWE on SMAD 2 and SMAD3 expressions and phosphorylations. Results are presented as means±SDs ($n \leq 5$). * $p \leq 0.05$, ** $p \leq 0.001$, *** $p \leq 0.0001$.

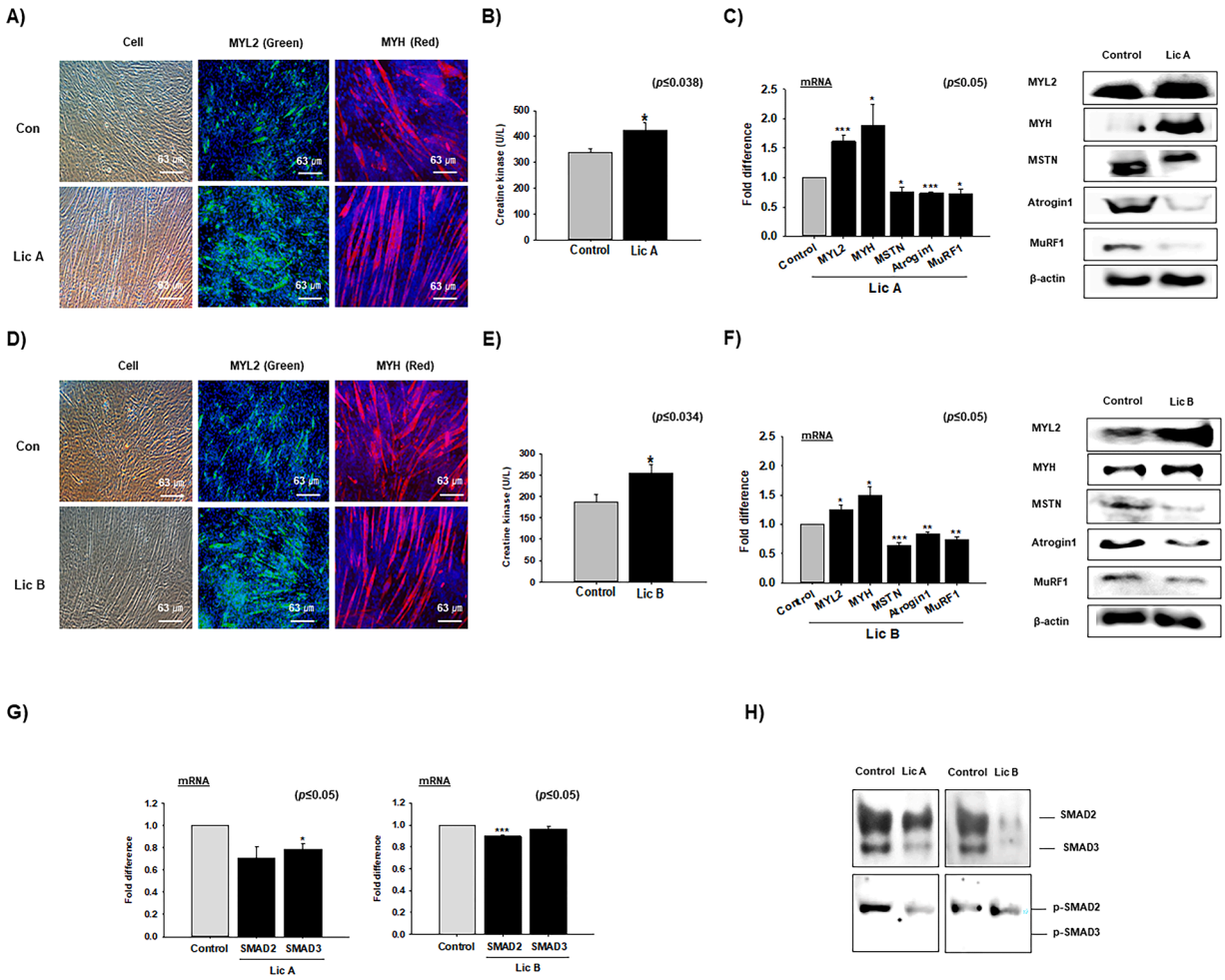

Fig. 6. Effects of Lic A and B on myoblast differentiation. C2C12 myoblasts were incubated in proliferation media until 70 % confluent. The medium was then replaced with differentiation media supplemented with Lic A or Lic B and cells were incubated for a further 4 days. (A) & (B) MYL2 and MYH protein expressions in non-treated and Lic A treated cells and myogenic differentiation were assessed immunocytochemically and using a creatine kinase assay, respectively. (C) MYL2, MYH, MSTN, Atrogin1, and MuRF1 mRNA and protein expressions were assessed by real time RT-PCR and Western blot, respectively, in non-treated and Lic A treated cells. (D), (E) MYL2 and MYH protein expressions and myogenic differentiation were assessed by immunocytochemistry and using a creatine kinase assay, respectively, in non-treated and Lic B treated cells. (F) MYL2, MYH, MSTN, Atrogin1, and MuRF1 mRNA and protein expressions were assessed by real time RT-PCR and Western blot, respectively in non-treated and Lic B treated cells. (G) & (H) Effects of Lic 2 and Lic 3 on the expressions and phosphorylations of SMAD 2 and SMAD3. Results are presented as means±SDs ($n \leq 5$). * $p \leq 0.05$, ** $p \leq 0.001$, *** $p \leq 0.0001$.

CWE, Lic A, and Lic B effects on aged cell proliferation

C2C12 cells were treated with ceramide for 2 days to induce aging and cell cycles were analyzed. Ceramide treatment increased the proportion of cells in the G0/G1 phase but decreased the proportion in the S/G2/M phase and suppressed proliferation (Supplementary Fig. 4A). In addition, ceramide reduced Ki67 and CyclinA2 expression and increased MSTN, Atrogin1, and MuRF1 expression (Supplementary Fig. 4B). After inducing cell aging, cells were treated with CWE, Lic A, or Lic B for 2 days (Fig. 7A). We found that CWE-treated aged cells proliferated more rapidly than aged non-treated cells (control). Furthermore, the mRNA and protein levels of MSTN, Atrogin1, and MuRF1 were lower in CWE, Lic A, or Lic B treated aged non-treated cells (control) (Fig. 7B–D). In addition, SMAD2 and SMAD3 expressions and phosphorylated SMAD 2 levels were lower in CWE, Lic A, and B-treated aged cells (Fig. 7E, F). Collectively these findings suggest that CWE, Lic A, and B might be effective anti- aging agents because they promoted cell proliferation and reduced MSTN levels and muscle atrophy marker levels in ceramide-induced aged cells.

Discussion

Aging, cachexia, and atrophy are the most common causes of muscle mass loss and few treatments are available that effectively address this condition (Huang et al., 2022). It has also been observed that muscle atrophy is a more critical factor in cancer cachexia development than fat loss (Dolly et al., 2020). Several studies have concluded that MSTN is a potential therapeutic target for preventing muscle mass loss in individuals with various muscle-wasting disorders and that MSTN contributes positively to muscle atrophy (Burch et al., 2017; Sartori et al., 2021). This study aimed to build upon our previous findings regarding the promotion of myoblast proliferation, differentiation, and muscle regeneration by *G. uralensis* (Lee et al., 2021c). We conducted *in silico, in vitro*, and *in vivo* studies to determine the impacts of the CWE and its main constituents, Lic A and B, on muscle mass regulation, MSTN expression, and the expressions of Atrogin 1 and MuRF1 (two atrophy-related genes). Chalcones (Lic A, B, C, D, E F, and G) are flavonoid precursors that possess two benzene rings linked by an α, β-unsaturated α-carbon ketone. These chalcones are found in licorice roots and have a wide range of health benefits due to their antibacterial,

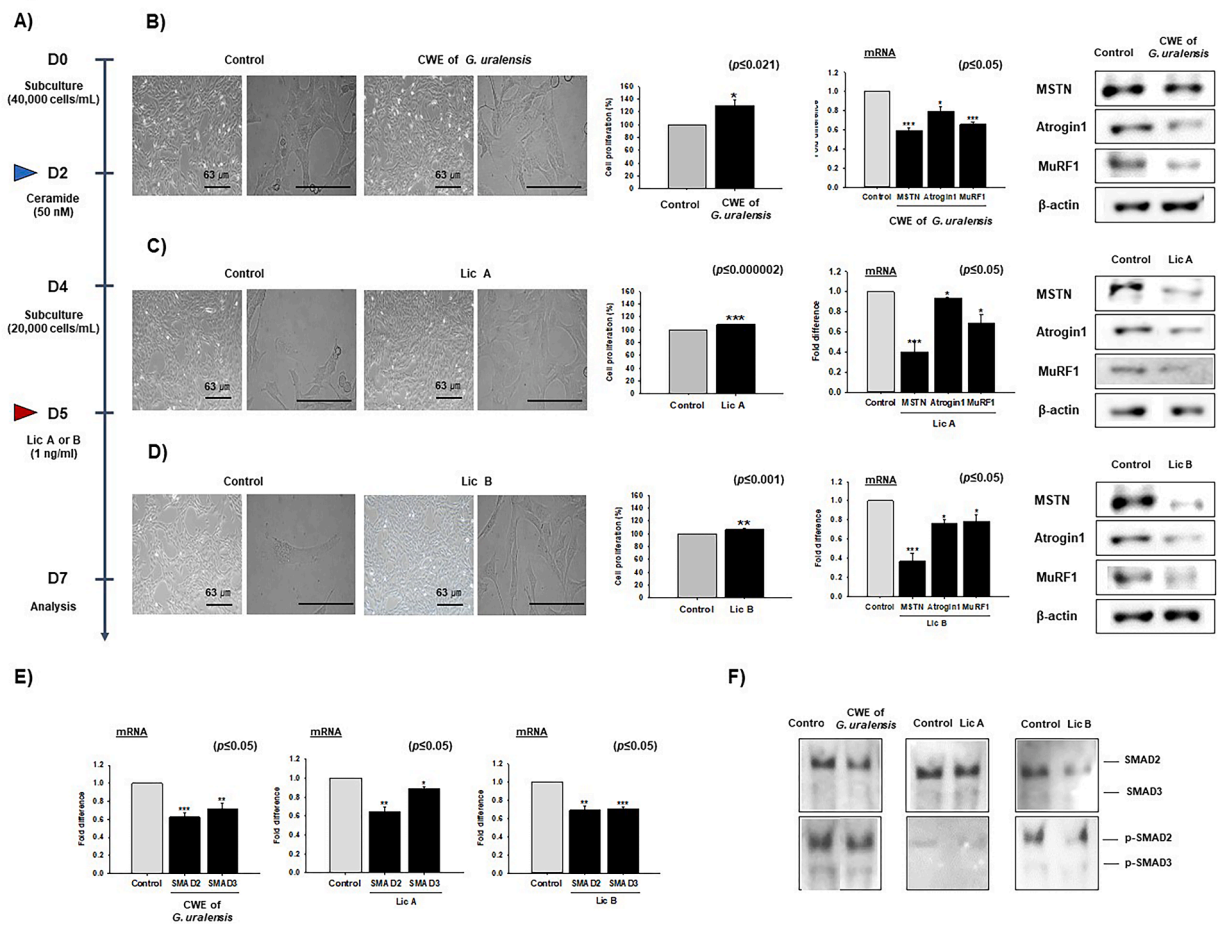

Fig. 7. Effects of CWE, Lic A, and Lic B on aged cells. (A) C2C12 cells were aged by incubation in proliferation media supplemented with 50 uM ceramide for 2 days and then sub-cultured in proliferation medium supplemented with CWE (100 ug/ml), Lic A, or Lic B (1 ng/ml) for 2 days. (B)–D) Cell proliferations of non-treated and treated cells were analyzed using an MTS assay. MSTN, Atrogin1, and MuRF1, mRNA and protein expressions were assessed by real time RT-PCR and Western blot. (E) , (F) Effects of CWE, Lic A, and Lic B on the expressions and phosphorylations of SMAD2 and SMAD3. Results are presented as means±SDs ($n \leq 5$). * $p \leq 0.05$, ** $p \leq 0.001$, *** $p \leq 0.0001$.

antioxidant, anti-inflammatory, and immunomodulatory properties (Maria Pia et al., 2019). In particular, Lic A has anti-aging properties attributed to the activation of the glycolysis pathway (Wu et al., 2021), and has been reported to have therapeutic potential for the treatment of obesity and nonalcoholic fatty liver disease by ameliorating weight gain and fatty liver disease and improving lipid metabolism via sirt1/AMPK pathway activation (Liou et al., 2019). Furthermore, utilizing *in silico* and *in vitro* studies, we recently discovered that Lic A and Lic B inhibit dipeptidyl peptidase-4 (DPP-4), an intriguing therapeutic target in type 2 diabetes mellitus (Shaikh et al., 2022).

In this study, we observed stable binding of Lic A, B, and C with MSTN through computational analysis, including molecular docking and MD simulation analysis. Furthermore, our *in vitro* and *in vivo* findings demonstrated that Lic A, B, and CWE significantly increased the muscle fiber diameter in mice, while reducing the expression of MSTN as well as the marker genes associated with muscle atrophy, namely Atrogin 1 and MuRF1. This study uniquely identified Lic A, B, and CWE as natural constituents with the potential to act as MSTN inhibitors. Consequently, they could be potential therapeutics for diseases associated with aging and muscle mass loss.

We observed that CWE, Lic A, and Lic B increased the muscle fiber diameter, which was in line with its suppressive effects on the expressions of MSTN and atrophy-related proteins. MSTN inhibition promotes muscular hypertrophy (Lee and McPherron, 2001; Lee, 2021). Furthermore, MSTN is known to negatively regulate the number of muscle fibers produced during their development and growth in adults (Haidet et al., 2008; Lee and McPherron, 2001), and multiple studies have concluded that MSTN inhibition is the most effective therapy for muscle mass regulation, muscular atrophy, sarcopenia, and other muscle-related ailments (Lee et al., 2022; Saitoh et al., 2017).

Previous research has demonstrated that inhibitors of signaling through the MSTN-ACVRIIB pathway have potential utilities as muscle-enhancing agents (Lee, 2021). Our *in silico* analysis revealed that Lic A, B, and C bind to the active site of MSTN and thus inhibit its binding to ACVRIIB. The molecular docking analysis was performed three times and the average value of binding energy as well as pKi was calculated. Compared to Lic A and B, the pKi value of Lic C was found to be significantly higher. The key residues of MSTN *viz.*, TRP 29, TRP 31, ASP 30, MET 84, MYR 86, PHE 87,GLU 9, MET 101 and others were found to be ineracted with Lic A, B and C. Specifically, TRP 31, MET 84, and TYR 86 were cruicial MSTN residues that interacted with Lic A; similarly, MET 101, GLY 89, and TRP 31 interacted with Lic B; and TRP 31, TYR 86, and MET 84 were cruicial amino acid residues that interacted with Lic C (Supplementary Fig. S5). Furthermore, it was ascertained that the three compounds' absorption, distribution, metabolism, excretion, and toxicity (ADMET) attributes, which are essential factors in small molecule drug discovery, were also predicted and determined to fall within acceptable ranges (Supplementary Table S3). The protein-protein docking of MSTN with its natural receptor, ACVRIIB, with and without Lic A, B, or C, demonstrated the effect of these compounds on MSTN binding efficacy with ACVRIIB. The results showed that in the presence of Lic A, B, and C, the global binding energy of MSTN with its

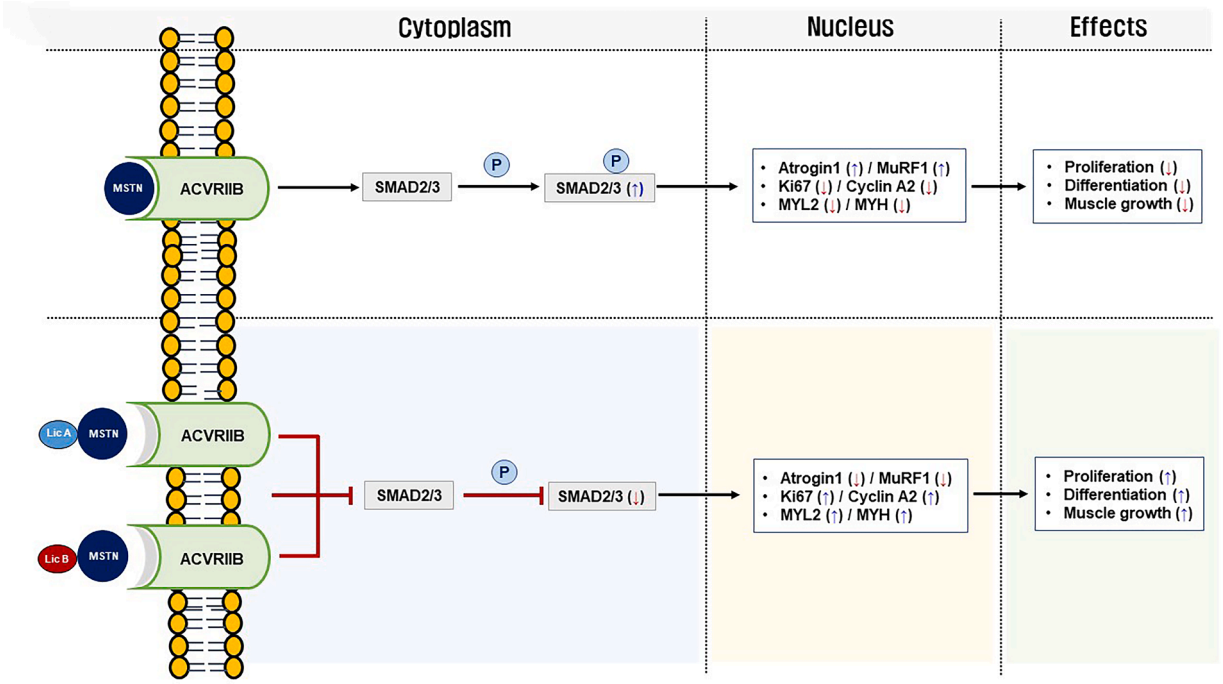

Fig. 8. Summary.

receptor (ACVRIIB) was reduced, implying that these compounds have the potential to be potent MSTN inhibitors.

Furthermore, protein-protein docking results showed that the global energy of the MSTN-ACVRIIB complex, as predicted by the FireDock web tool, was diminished in the presence of Lic A, Lic B, or Lic C, and 100 ns MD simulations showed all three stably bind to MSTN. In addition, our observations revealed that Lic A and B formed 2–4 H bonds with MSTN, while Lic C formed only 1, –2 H bonds, which concurs with the results of our previous computational studies that natural compounds bind to MSTN (Ali et al., 2022) and inhibit its signaling via ACVRIIB (Ahmad et al., 2021; Baig et al., 2017). However, in the case of Lic C, we noticed inconsistencies between *in silico* and *in vitro* results since molecular docking analysis showed it binds strongly to MSTN but *in vitro* showed that, unlike Lic A and B, it reduced myoblast cell proliferation and differentiation. On the other hand, simulation analysis showed Lic C formed fewer H bonds with MSTN, suggesting greater instability of the Lic C-MSTN complex.

The murine study revealed that treatment with CWE significantly reduced plasma MSTN concentrations, which in combination with its downregulation of atrophy-related genes, implied that CWE may have contributed to the observed increases in muscle fiber diameters. In addition, CWE promoted muscle regeneration by downregulating muscle atrophy-associated proteins and genes and upregulating genes involved in muscle cell growth. More specifically, CWE, Lic A, and Lic B significantly downregulated the mRNA and protein levels of MSTN, Atrogin 1, and MuRF1 but significantly upregulated MYH. These observations suggest that CWE positively influenced MSC differentiation and potentially muscle regeneration by preventing muscle cell atrophy and promoting the growth of new muscle cells. These results are in line with those of Yasukiyo Yoshioka et al., who determined that the administration of licorice flavonoid oil in KK-A^y/Ta mice leads to an increase in muscle mass. This effect is achieved by downregulating muscle atrophy markers, activating the mTOR and p70 S6K pathways, and regulating FoxO3a phosphorylation (Yoshioka et al., 2018). These results also support previous reports on the beneficial effects of *G. uralensis* extract on TNF-α-induced muscle atrophy attributed to its downregulations of muscle atrophy markers, NF-κB phosphorylation, and Smad3 proteins, its upregulation of MYH, and its promotion of Nrf2 translocation for antioxidant and apoptosis-related regulation (Choi et al., 2022).

Furthermore, CWE, Lic A, and Lic B significantly increased in protein and mRNA expressions of the cell proliferation markers, Ki67 and Cyclin A2, in C2C12 cells. Ki67 is strongly associated with the proliferation of somatic cells and is widely utilized as a proliferation marker and to estimate active myoblast proliferation (Sun and Kaufman, 2018). On the other hand, Cyclin A2 regulates cell cycle progression and coordinates G1 to S phase transition. Cyclin A2 expression is typically elevated in proliferating myoblasts during myogenesis, and this upregulation is associated with significant downregulations of MSTN, Atrogin1, and MuRF1 (De Falco and De Luca, 2006). Moreover, Cyclin A2 also reduced the expressions of SMAD 2 and 3 and their phosphorylations. Phosphorylated SMAD 2 and 3 are transcriptional activators of MuRF1, and SMAD 2 and 3 are signaling molecules downstream of TGF-β and MSTN. Furthermore, the TGF-β/SMAD3 pathway has a detrimental effect on muscle mass. Also, the activations of SMAD 2 and 3 increase the expressions of FoxO1 and FoxO3, and thus, upregulate markers of muscle atrophy (Sartori et al., 2021). The observed significant downregulations of MSTN by CWE, Lic A, or B provide a convincing rationale for declines in the expressions SMAD 2 and 3. Thus, our findings suggest that CWE, Lic A, and B promote cell proliferation by downregulating the expressions of MSTN and atrophy genes and simultaneously upregulating the expressions of proliferation markers at the protein and mRNA levels.

In addition, it was discovered that Lic A and Lic B promote muscle differentiation. Both significantly increased MYL2 and MYH (myogenic markers), creatine kinase, and myotube formation, while decreasing MSTN, Atrogin1, MuRF1, and SMAD 2 and 3. The inhibitory function of MSTN on myoblast differentiation is well described, with SMAD 3 serving as a mediator of this inhibitory process (Langley et al., 2002). These findings are also in line with our earlier findings, which showed that Lic B promotes myoblast proliferation and differentiation (Lee et al., 2021c).

After confirming the effects of CWE, Lic A, and Lic B on muscle fiber diameter, muscle mass regulation, and C2C12 and mouse primary MSCs proliferation, and differentiation, we investigated their effects on ceramide-induced aged C2C12 cells. CWE, Lic A, and Lic B increased the proliferation of aged cells. On the other hand, they reduced the

expressions of MSTN, Atrogin1, and MuRF1 at the mRNA and protein levels. Atrogin-1 and MuRF1 are E3 ubiquitin ligases that control ubiquitin-mediated protein degradation in SM, and increases in their levels are related to the onset of muscle atrophy (Bodine and Baehr, 2014). In addition, CWE, Lic A, and Lic B reduced the expressions of SMAD2 and SMAD3 and their phosphorylated forms. SMAD2 and SMAD3 are signaling molecules that transmit signals from cell surface receptors to nuclei, regulating MSTN expression and initiating a signaling cascade that phosphorylates SMAD2 and SMAD3 (Zhu et al., 2004). CWE, Lic A, and B impeded the triggering and transduction of MSTN signaling by decreasing SMAD2 and SMAD3 expressions and their phosphorylations. Our findings that CWE, Lic A, and Lic B increased cell proliferation and downregulated MSTN and its downstream signaling molecules, and muscle atrophy-associated genes in aged cells suggest that they have anti-aging properties, which is in line with previous reports that licorice has antioxidant and anti-aging effects *in vitro* and *in vivo* (Reigada et al., 2020; Zhao et al., 2018). These findings are also consistent with the findings of Wu et al., who discovered that Lic A has anti-aging properties by activating the glycolysis pathway (Wu et al., 2021).

The present study shows that the CWE and two of its active constituents Lic A and B support muscle growth, prevent muscle atrophy, promote muscle regeneration, and mitigate the effects of cell aging. Furthermore, our *in silico* and *in vitro* experiments showed CWE, Lic A, and Lic B exhibit muscle-enhancing effects including increased cell proliferation and muscle differentiation and reduced the expressions of muscle atrophy markers and important signaling pathways components, like SMAD2 and SMAD3 (Fig. 8). Collectively, the findings indicate that the CWE and its active constituents could be used as an anti-muscle aging agent as well as in the treatment of muscle-related diseases. In particular, they were found to be potent MSTN inhibitors and candidate treatments for muscle wasting disorders.

Authors contributions

All data were generated in-house, and no paper mill was used. All authors agree to be accountable for all aspects of work ensuring integrity and accuracy.

CRediT authorship contribution statement

Khurshid Ahmad: Writing – original draft, Writing – review & editing, Investigation, Data curation, Methodology, Formal analysis. **Eun Ju Lee:** Writing – review & editing, Funding acquisition, Validation, Conceptualization, Methodology, Investigation, Formal analysis, Writing – original draft, Data curation. **Shahid Ali:** Visualization, Software, Formal analysis. **Ki Soo Han:** Writing – review & editing, Methodology, Validation, Resources, Investigation. **Sun Jin Hur:** Writing – review & editing, Data curation. **Jeong Ho Lim:** Writing – review & editing, Investigation, Methodology, Formal analysis. **Inho Choi:** Writing – review & editing, Supervision, Project administration, Formal analysis, Funding acquisition, Conceptualization.

Declaration of competing interest

None.

Acknowledgment

This research was supported by the Basic Science Research Program of the National Research Foundation of Korea (NRF), funded by the Ministry of Education (2020R1A6A1A03044512), the National Research Foundation of Korea (NRF), and the Korean Government (NRF-2021R1A2C2004177). In addition, the study was supported by the Forestry (IPET) through High Value-added Food Technology Development Program of the Korea Institute of Planning and Evaluation for Technology in Food and Agriculture funded by the Ministry of Agriculture, Food, and Rural Affairs (MAFRA) (Grant No's. 321026-05 and 322008-5).

Supplementary materials

Supplementary material associated with this article can be found, in the online version, at doi:10.1016/j.phymed.2024.155350.

References

Abati, E., Manini, A., Comi, G.P., Corti, S., 2022. Inhibition of Myostatin and related signaling pathways for the treatment of muscle atrophy in motor neuron diseases. Cell. Mol. Life Sci. CMLS 79, 374.

Ahmad, K., Shaikh, S., Lim, J.H., Ahmad, S.S., Chun, H.J., Lee, E.J., Choi, I., 2023. Therapeutic application of natural compounds for skeletal muscle-associated metabolic disorders: a review on diabetes perspective. Biomed. Pharmacother. 168, 115642.

Ahmad, S.S., Ahmad, K., Lee, E.J., Shaikh, S., Choi, I., 2021. Computational identification of dithymoquinone as a potential inhibitor of Myostatin and regulator of muscle mass. Molecules 26, 5407.

Ali, S., Ahmad, K., Shaikh, S., Lim, J.H., Chun, H.J., Ahmad, S.S., Lee, E.J., Choi, I., 2022. Identification and evaluation of traditional chinese medicine natural compounds as potential Myostatin inhibitors: an *in silico* approach. Molecules 27, 4303.

Argilés, J.M., Busquets, S., Felipe, A., López-Soriano, F.J., 2006. Muscle wasting in cancer and ageing: cachexia *versus* sarcopenia. Adv. Gerontol. Uspekhi Gerontol. 18, 39–54.

Asl, M.N., Hosseinzadeh, H., 2008. Review of pharmacological effects of Glycyrrhiza sp. and its bioactive compounds. Phytother. Res. 22, 709–724.

Atanasov, A.G., Zotchev, S.B., Dirsch, V.M., Supuran, C.T., 2021. Natural products in drug discovery: advances and opportunities. Nat. Rev. Drug Discov. 20, 200–216.

Ayeka, P.A., Bian, Y., Mwitari, P.G., Chu, X., Zhang, Y., Uzayisenga, R., Otachi, E.O., 2016. Immunomodulatory and anticancer potential of Gan cao (*Glycyrrhiza uralensis* Fisch.) polysaccharides by CT-26 colon carcinoma cell growth inhibition and cytokine IL-7 upregulation *in vitro*. BMC Complement. Altern. Med. 16, 206.

Baig, M.H., Ahmad, K., Moon, J.S., Park, S.Y., Ho Lim, J., Chun, H.J., Qadri, A.F., Hwang, Y.C., Jan, A.T., Ahmad, S.S., 2022. Myostatin and its regulation: a comprehensive review of Myostatin inhibiting strategies. Front. Physiol. 13, 876078.

Baig, M.H., Jan, A.T., Rabbani, G., Ahmad, K., Ashraf, J.M., Kim, T., Min, H.S., Lee, Y.H., Cho, W.K., Ma, J.Y., 2017. Methylglyoxal and advanced glycation end products: insight of the regulatory machinery affecting the myogenic program and of its modulation by natural compounds. Sci. Rep. 7, 5916.

Bodine, S.C., Baehr, L.M., 2014. Skeletal muscle atrophy and the E3 ubiquitin ligases MuRF1 and MAFbx/atrogin-1. American journal of physiology. Endocrinol. Metab. 307, E469–E484.

Burch, P.M., Pogoryelova, O., Palandra, J., Goldstein, R., Bennett, D., Fitz, L., Guglieri, M., Bettolo, C.M., Straub, V., Evangelista, T., Neubert, H., Lochmüller, H., Morris, C., 2017. Reduced serum Myostatin concentrations associated with genetic muscle disease progression. J. Neurol. 264, 541–553.

Choi, J.W., Choi, S.Y., Lee, H.H.L., Yoo, G., Lee, S.H., Choi, I.W., Cho, C.H., Hur, J., 2022. *Glycyrrhiza uralensis* attenuates TNF-α-induced muscle atrophy in myoblast cells through the Nrf2 and MAFbx signaling cascades. Appl. Biol. Chem. 65, 1–12.

Chu, C., Deng, J., Hou, Y., Xiang, L., Wu, Y., Qu, Y., Man, Y., 2017a. Application of PEG and EGCG modified collagen-base membrane to promote osteoblasts proliferation. Mater. Sci. Eng. C 76, 31–36.

Chu, C., Deng, J., Man, Y., Qu, Y., 2017b. Green tea extracts epigallocatechin-3-gallate for different treatments. Biomed .Res. Int. 2017, 5615647.

Chu, C., Wang, Y., Wang, Y., Yang, R., Liu, L., Rung, S., Xiang, L., Wu, Y., Du, S., Man, Y., 2019. Evaluation of epigallocatechin-3-gallate (EGCG) modified collagen in guided bone regeneration (GBR) surgery and modulation of macrophage phenotype. Mater. Sci. Eng. C 99, 73–82.

De Falco, M., De Luca, A., 2006. Involvement of cdks and cyclins in muscle differentiation. Eur. J. Histochem. 50, 19–23.

Dolly, A., Dumas, J.F., Servais, S., 2020. Cancer cachexia and skeletal muscle atrophy in clinical studies: what do we really know? J. Cachexia Sarcopenia Muscle 11, 1413–1428.

Fan, H., Zhang, R., Tesfaye, D., Tholen, E., Looft, C., Hölker, M., Schellander, K., Cinar, M.U., 2012. Sulforaphane causes a major epigenetic repression of Myostatin in porcine satellite cells. Epigenetics 7, 1379–1390.

Furrer, R., Handschin, C., 2019. Muscle wasting diseases: novel targets and treatments. Annu. Rev. Pharmacol. Toxicol. 59, 315–339.

Gutierrez-Salmean, G., Ciaraldi, T.P., Nogueira, L., Barboza, J., Taub, P.R., Hogan, M.C., Henry, R.R., Meaney, E., Villarreal, F., Ceballos, G., Ramirez-Sanchez, I., 2014. Effects of (-)-epicatechin on molecular modulators of skeletal muscle growth and differentiation. J. Nutr. Biochem. 25, 91–94.

Haidet, A.M., Rizo, L., Handy, C., Umapathi, P., Eagle, A., Shilling, C., Boue, D., Martin, P.T., Sahenk, Z., Mendell, J.R., 2008. Long-term enhancement of skeletal muscle mass and strength by single gene administration of Myostatin inhibitors. Proc. Natl. Acad. Sci. 105, 4318–4322.

Hata, A., Chen, Y.G., 2016. TGF-β signaling from receptors to Smads. Cold Spring Harb. Perspect. Biol. 8, a022061.

Hernández-Hernández, J.M., García-González, E.G., Brun, C.E., Rudnicki, M.A., 2017. The myogenic regulatory factors, determinants of muscle development, cell identity and regeneration. Seminars in Cell & Developmental Biology. Elsevier, pp. 10-18.
Huang, L., Li, M., Deng, C., Qiu, J., Wang, K., Chang, M., Zhou, S., Gu, Y., Shen, Y., Wang, W., Huang, Z., Sun, H., 2022. Potential therapeutic strategies for skeletal muscle atrophy. Antioxidants 12, 44.
Humphrey, W., Dalke, A., Schulten, K., 1996. VMD: visual molecular dynamics. J. Mol. Graph. 14, 27–38, 33-38.
Kim, J.W., Ku, S.K., Han, M.H., Kim, K.Y., Kim, S.G., Kim, G.Y., Hwang, H.J., Kim, B.W., Kim, C.M., Choi, Y.H., 2015. The administration of Fructus Schisandrae attenuates dexamethasone-induced muscle atrophy in mice. Int. J. Mol. Med. 36, 29–42.
Kuang, S., Gillespie, M.A., Rudnicki, M.A., 2008. Niche regulation of muscle satellite cell self-renewal and differentiation. Cell Stem Cell 2, 22–31.
Langley, B., Thomas, M., Bishop, A., Sharma, M., Gilmour, S., Kambadur, R., 2002. Myostatin inhibits myoblast differentiation by down-regulating MyoD expression. J. Biol. Chem. 277, 49831–49840.
Lee, E.J., Ahmad, K., Pathak, S., Lee, S., Baig, M.H., Jeong, J.H., Doh, K.O., Lee, D.M., Choi, I., 2021a. Identification of novel FNIN2 and FNIN3 fibronectin-derived peptides that promote cell adhesion, proliferation and differentiation in primary cells and stem cells. Int. J. Mol. Sci. 22, 3042.
Lee, E.J., Ahmad, S.S., Lim, J.H., Ahmad, K., Shaikh, S., Lee, Y.S., Park, S.J., Jin, J.O., Lee, Y.H., Choi, I., 2021b. Interaction of fibromodulin and Myostatin to regulate skeletal muscle aging: an opposite regulation in muscle aging, diabetes, and intracellular lipid accumulation. Cells 10, 2083.
Lee, E.J., Jan, A.T., Baig, M.H., Ahmad, K., Malik, A., Rabbani, G., Kim, T., Lee, I.K., Lee, Y.H., Park, S.Y., Choi, I., 2018. Fibromodulin and regulation of the intricate balance between myoblast differentiation to myocytes or adipocyte-like cells. FASEB J. 32, 768–781.
Lee, E.J., Shaikh, S., Ahmad, K., Ahmad, S.S., Lim, J.H., Park, S., Yang, H.J., Cho, W.K., Park, S.J., Lee, Y.H., 2021c. Isolation and characterization of compounds from *Glycyrrhiza uralensis* as therapeutic agents for the muscle disorders. Int. J. Mol. Sci. 22, 876.
Lee, E.J., Shaikh, S., Baig, M.H., Park, S.Y., Lim, J.H., Ahmad, S.S., Ali, S., Ahmad, K., Choi, I., 2022. MIF1 and MIF2 Myostatin peptide inhibitors as potent muscle mass regulators. Int. J. Mol. Sci. 23, 4222.
Lee, E.J., Shaikh, S., Choi, D., Ahmad, K., Baig, M.H., Lim, J.H., Lee, Y.H., Park, S.J., Kim, Y.W., Park, S.Y., Choi, I., 2019. Transthyretin maintains muscle homeostasis through the novel shuttle pathway of thyroid hormones during myoblast differentiation. Cells 8, 1565.
Lee, S.J., Bhasin, S., Klickstein, L., Krishnan, V., Rooks, D., 2023. Challenges and future prospects of targeting Myostatin/activin A signaling to treat diseases of muscle loss and metabolic dysfunction. J. Gerontol. Ser. A 78, 32–37.
Lee, S.J., McPherron, A.C., 2001. Regulation of Myostatin activity and muscle growth. Proc. Natl. Acad. Sci. 98, 9306–9311.
Lee, S.J., 2021. Targeting the Myostatin signaling pathway to treat muscle loss and metabolic dysfunction. J. Clin. Investig. 131, 9.
Liou, C.J., Lee, Y.K., Ting, N.C., Chen, Y.L., Shen, S.C., Wu, S.J., Huang, W.C., 2019. Protective effects of licochalcone A ameliorates obesity and non-alcoholic fatty liver disease via promotion of the Sirt-1/AMPK pathway in mice fed a high-fat diet. Cells 8, 447.
Liu, D., Qiao, X., Ge, Z., Shang, Y., Li, Y., Wang, W., Chen, M., Si, S., Chen, S.Z., 2019. IMB0901 inhibits muscle atrophy induced by cancer cachexia through MSTN signaling pathway. Skelet. Muscle 9, 1–14.
Liu, M., Qin, J., Hao, Y., Liu, M., Luo, J., Luo, T., Wei, L., 2013. Astragalus polysaccharide suppresses skeletal muscle Myostatin expression in diabetes: involvement of ROS-ERK and NF-κB pathways. Oxid Med. Cell. Longev. 2013, 782497.
Mafi, F., Biglari, S., Ghardashi Afousi, A., Gaeini, A.A., 2019. Improvement in skeletal muscle strength and plasma levels of follistatin and Myostatin induced by an 8-Week resistance training and epicatechin supplementation in sarcopenic older adults. J. Aging Phys. Act. 27, 384–391.
Maria Pia, G.D., Sara, F., Mario, F., Lorenza, S., 2019. Biological effects of licochalcones. Mini Rev. Med. Chem. 19, 647–656.
Mashiach, E., Schneidman-Duhovny, D., Andrusier, N., Nussinov, R., Wolfson, H.J., 2008. FireDock: a web server for fast interaction refinement in molecular docking. Nucleic Acids Res. 36, W229–W232.
Miura, T., Kishioka, Y., Wakamatsu, J., Hattori, A., Nishimura, T., 2010. Interaction between Myostatin and extracellular matrix components. Anim. Sci. J. 81, 102–107.
Morris, G.M., Huey, R., Lindstrom, W., Sanner, M.F., Belew, R.K., Goodsell, D.S., Olson, A.J., 2009. AutoDock4 and AutoDockTools4: automated docking with selective receptor flexibility. J. Comput. Chem. 30, 2785–2791.
Mukund, K., Subramaniam, S., 2020. Skeletal muscle: a review of molecular structure and function, in health and disease. Wiley Interdiscip. Rev. Syst. Biol. Med. 12, e1462.
Newman, D.J., Cragg, G.M., 2012. Natural products as sources of new drugs over the 30 years from 1981 to 2010. J. Nat. Prod. 75, 311–335.
Pang, K.T., Loo, L.S.W., Chia, S., Ong, F.Y.T., Yu, H., Walsh, I., 2023. Insight into muscle stem cell regeneration and mechanobiology. Stem Cell Res. Ther. 14, 129.
Pol-Fachin, L., Fernandes, C.L., Verli, H., 2009. GROMOS96 43a1 performance on the characterization of glycoprotein conformational ensembles through molecular dynamics simulations. Carbohydr. Res. 344, 491–500.
Reigada, I., Moliner, C., Valero, M.S., Weinkove, D., Langa, E., Gómez Rincón, C., 2020. Antioxidant and antiaging effects of licorice on the caenorhabditis elegans model. J. Med. Food 23, 72–78.
Rybalka, E., Timpani, C.A., Debruin, D.A., Bagaric, R.M., Campelj, D.G., Hayes, A., 2020. The failed clinical story of Myostatin inhibitors against duchenne muscular dystrophy: exploring the biology behind the battle. Cells 9, 2657.
Saitoh, M., Ishida, J., Ebner, N., Anker, S.D., Springer, J., von Haehling, S., 2017. Myostatin inhibitors as pharmacological treatment for muscle wasting and muscular dystrophy. JCSM Clin. Rep. 2, 1–10.
Sartori, R., Romanello, V., Sandri, M., 2021. Mechanisms of muscle atrophy and hypertrophy: implications in health and disease. Nat. Commun. 12, 330.
Schneider, C.A., Rasband, W.S., Eliceiri, K.W., 2012. NIH image to ImageJ: 25 years of image analysis. Nat. Methods 9, 671–675.
Schneidman-Duhovny, D., Inbar, Y., Nussinov, R., Wolfson, H.J., 2005. PatchDock and SymmDock: servers for rigid and symmetric docking. Nucleic Acids Res. 33, W363–W367.
Shaikh, S., Ali, S., Lim, J.H., Chun, H.J., Ahmad, K., Ahmad, S.S., Hwang, Y.C., Han, K.S., Kim, N.R., Lee, E.J., 2022. Dipeptidyl peptidase-4 inhibitory potentials of *Glycyrrhiza uralensis* and its bioactive compounds licochalcone A and licochalcone B: an in silico and *in vitro* study. Front. Mol. Biosci. 9, 1024764.
Sousa-Victor, P., García-Prat, L., Muñoz-Cánoves, P., 2022. Control of satellite cell function in muscle regeneration and its disruption in ageing. Nat. Rev. Mol. Cell Biol. 23, 204–226.
St Andre, M., Johnson, M., Bansal, P.N., Wellen, J., Robertson, A., Opsahl, A., Burch, P. M., Bialek, P., Morris, C., Owens, J., 2017. A mouse anti-Myostatin antibody increases muscle mass and improves muscle strength and contractility in the mdx mouse model of Duchenne muscular dystrophy and its humanized equivalent, domagrozumab (PF-06252616), increases muscle volume in cynomolgus monkeys. Skelet. Muscle 7, 1–12.
Suh, J., Lee, Y.S., 2020. Myostatin inhibitors: panacea or predicament for musculoskeletal disorders? J. Bone Metab. 27, 151.
Sun, X., Kaufman, P.D., 2018. Ki-67: more than a proliferation marker. Chromosoma 127, 175–186.
Thomas, M., Langley, B., Berry, C., Sharma, M., Kirk, S., Bass, J., Kambadur, R., 2000. Myostatin, a negative regulator of muscle growth, functions by inhibiting myoblast proliferation. J. Biol. Chem. 275, 40235–40243.
Van Der Spoel, D., Lindahl, E., Hess, B., Groenhof, G., Mark, A.E., Berendsen, H.J., 2005. GROMACS: fast, flexible, and free. J. Comput. Chem. 26, 1701–1718.
Welle, S., Cardillo, A., Zanche, M., Tawil, R., 2009. Skeletal muscle gene expression after Myostatin knockout in mature mice. Physiol. Genom. 38, 342–350.
Wu, Y., Wang, H., Zhu, J., Shen, H., Liu, H., 2021. Licochalcone A activation of glycolysis pathway has an anti-aging effect on human adipose stem cells. Aging 13, 25180–25194.
Yin, H., Price, F., Rudnicki, M.A., 2013. Satellite cells and the muscle stem cell niche. Physiol. Rev. 93, 23–67.
Yoshioka, Y., Yamashita, Y., Kishida, H., Nakagawa, K., Ashida, H., 2018. Licorice flavonoid oil enhances muscle mass in KK-Ay mice. Life Sci. 205, 91–96.
Yuan, S., Chan, H.S., Hu, Z., 2017. Using PyMOL as a platform for computational drug design. Wiley Interdiscip. Rev. Comput. Mol. Sci. 7, e1298.
Zhao, F., Gao, L., Qin, X., Du, G., Zhou, Y., 2018. The intervention effect of licorice in D-galactose induced aging rats by regulating the taurine metabolic pathway. Food Funct. 9, 4814–4821.
Zhu, X., Topouzis, S., Liang, L.F., Stotish, R.L., 2004. Myostatin signaling through Smad2, Smad3 and Smad4 is regulated by the inhibitory Smad7 by a negative feedback mechanism. Cytokine 26, 262–272.